

## Role of spin-orbit strength in the prediction of closed shells in superheavy nuclei

A. N. Bezbakh, G. G. Adamian , and N. V. Antonenko  
 Joint Institute for Nuclear Research, 141980 Dubna, Russia



(Received 19 January 2022; revised 31 March 2022; accepted 2 May 2022; published 11 May 2022)

Using the microscopic-macroscopic approach based on the modified two-center shell model, the ground-state shell corrections are analyzed as a function of spin-orbit strength for even- $Z$  superheavy nuclei in the  $\alpha$ -decay chains containing <sup>295–300,302,304</sup>120 nuclei. The influence of the spin-orbit strength on the positions of shell closures and the description of the low-lying one-quasiparticle spectra for <sup>251</sup>Cf, <sup>243</sup>Cm, <sup>243</sup>Bk, and <sup>251</sup>Es nuclei are studied in detail. The importance of studying the nuclear structure of actinides for predicting the next double magic nucleus beyond <sup>208</sup>Pb is demonstrated.

DOI: [10.1103/PhysRevC.105.054305](https://doi.org/10.1103/PhysRevC.105.054305)

### I. INTRODUCTION

Experiments on complete fusion reactions with a <sup>48</sup>Ca beam and various actinide targets were successfully carried out at JINR (Dubna), GSI (Darmstadt), and LBNL (Berkeley) in order to synthesize superheavy nuclei (SHN) with the charge numbers  $Z = 112$ – $118$  [1–10]. The SHN with  $Z = 112$  and  $113$  were also produced at GSI (Darmstadt) and RIKEN (Tokyo) in cold fusion reactions with target nuclei <sup>208</sup>Pb and <sup>209</sup>Bi [11,12]. The new Superheavy Elements Factory at JINR opens up new possibilities in SHN research [3,13]. So the study of the physical (the nuclear structure, the location of the shell closures, and the decay modes) and chemical properties of superheavy elements, as well as of the synthesis of new SHN, are of interest. A theoretical analysis is required to guide experimental studies of the heaviest nuclei. Existing microscopic-macroscopic (MM) approaches [14–17] and self-consistent mean-field approaches [18–22] provide the basis for intensive calculations of the properties of heavy nuclei. However, a hitherto unsolved controversy of SHN physics is that the MM approaches [14–17] mainly locate the proton shell closure at flerovium (Fl,  $Z = 114$ ) while the nonrelativistic and relativistic self-consistent approaches predict stronger shell effect at  $Z = 120$ – $126$ . As found in Refs. [17,23,24], in the MM approach based on the modified two-center shell model (TCSM) [25] the proton shell closure can drift from  $Z = 114$  to  $Z = 120$  when adjusting slightly the nuclear mean field where spin-orbit interactions are of paramount importance for shell closures. The parameters of the TCSM were set to describe the spins and parities of the ground state and  $Q_\alpha$  values of the known heavy nuclei. The phenomenological model [26] relies on the  $Z = 126$  closed shell. Since nuclear models contain a number of parameters which are fixed for the best description of known nuclei, their predictive power may be less for nuclei that are far from the well-studied region of the nuclear chart. To improve the quality of predictions, one can specially adjust the parameters for describing the known properties of shell-stabilized nuclei close to the region of interest. We expect the difference in

the predicted shell closures in SHN to be mainly caused by different central mean-field and spin-orbit potentials used.

The aim of the present paper is to investigate the role spin-orbit strength in the region of SHN by using the MM approach [17,23,24]. The position of the proton shell closure in SHN seems to be more sensitive to spin-orbit interaction rather than central mean-field potential [27–29]. The spin-orbit potential predestines if the proton shell is located at  $Z = 114$  or  $120$  or  $126$ . We start with the spin-orbit strength adopted in Refs. [17,23,24] to describe the low-lying quasiparticle states in even-odd heavy nuclei for which the experimental data are available. This spin-orbit strength results in proton shell closure at  $Z = 120$  and not at  $Z = 114$ , as in other MM approaches. In this paper, we will show how this strength should be changed to shift the proton shell closure to  $Z = 114$  and  $Z = 126$ . The change of the quality of description of one-quasiparticle spectra will be presented with variation of the spin-orbit strength.

### II. MODEL

The single-particle Hamiltonian of the TCSM in the cylinder coordinates  $z, \rho, \phi$  is written as

$$H = -\frac{\hbar}{2m}\nabla^2 + V(\rho, z) + V_{ls} + V_{\rho^2}. \quad (1)$$

The shape of a nucleus is presented as two joined ellipsoids with the semiaxes  $a$  and  $b$  and the centers at  $z_1$  and  $z_2$ ,  $z_1 = -z_2$ . The momentum-independent part of the Hamiltonian is

$$V(\rho, z) = \begin{cases} \frac{1}{2}m\omega_z^2(z - z_1)^2 + \frac{1}{2}m\omega_\rho^2\rho^2, & z < z_1, \\ \frac{1}{2}m\omega_\rho^2\rho^2, & z_1 < z < z_2, \\ \frac{1}{2}m\omega_z^2(z - z_2)^2 + \frac{1}{2}m\omega_\rho^2\rho^2, & z > z_2, \end{cases}$$

where  $m$  is a nucleon mass,  $\omega_\rho/\omega_z = a/b = \beta$ , and  $z_2 - z_1 = 2R_0\lambda - 2a$ . Here,  $\omega_\rho = \beta\omega_0R_0/a$ ,  $\hbar\omega_0 = 41A^{-1/3}$  MeV, and  $R_0 = 1.2249A^{1/3}$  fm. The dimensionless parameters  $\lambda$  and  $\beta$  are related to  $a$  and  $b$  through the condition of volume conservation.

The momentum-dependent part of the Hamiltonian (1) consists of the spin-orbital term

$$V_{ls} = -\frac{2\hbar\kappa}{m\omega'_0}(\nabla V \times \mathbf{p})\mathbf{s} \quad (2)$$

and the  $l^2$  term

$$V_{l^2} = -\kappa\mu\hbar\omega'_0 l^2 + \kappa\mu\hbar\omega'_0 \frac{N(N+3)}{2} \delta_{if}. \quad (3)$$

Here  $\delta_{if}$  is a purely diagonal operator,  $N$  is the principal quantum number of the spherical oscillator,  $\hbar\omega'_0 = 41A'^{-1/3}$  MeV, and  $A' = Aab^2/R_0^3$ .

The terms  $V_{ls}$  and  $V_{l^2}$  (see Ref. [25]) contain the parameters  $\kappa_{n,p}$  and  $\mu_{n,p}$ , respectively. In Eqs. (2) and (3), the indices  $n, p$  are skipped for brevity. In order to improve the description of spins and parities of the nuclear ground states, we introduce a weak dependence on  $(N - Z)$  in the parameters  $\kappa_{n,p}$  and  $\mu_{n,p}$ . For the actinide and transactinide region we suggest [24]

$$\begin{aligned} \kappa_n &= -0.076 + 0.0058(N - Z) - 6.53 \times 10^{-5}(N - Z)^2 \\ &\quad + 0.002A^{1/3}, \\ \mu_n &= 1.598 - 0.0295(N - Z) + 3.036 \times 10^{-4}(N - Z)^2 \\ &\quad - 0.095A^{1/3} \end{aligned} \quad (4)$$

for neutrons and

$$\begin{aligned} \kappa_p &= 0.0383 + 0.00137(N - Z) - 1.22 \times 10^{-5}(N - Z)^2 \\ &\quad - 0.003A^{1/3}, \\ \mu_p &= 0.335 + 0.01(N - Z) - 9.367 \times 10^{-5}(N - Z)^2 \\ &\quad + 0.003A^{1/3} \end{aligned} \quad (5)$$

for protons. If Eqs. (4) lead to  $\kappa_n < 0.045 + 0.002A^{1/3}$ , we set  $\kappa_n = 0.045 + 0.002A^{1/3}$ . With the Nilsson-type single-particle potential the weak dependence on  $N - Z$  is incorporated into the momentum-dependent part of the single-particle Hamiltonian. With Eqs. (4) and (5) we are able to describe correctly the ground-state spins of many heavy nuclei treated. Note that the introduced additional dependence on  $N - Z$  mainly supplies a better order of the single-particle levels near the Fermi surface.

With the TCSM the potential energy is calculated as a sum of two terms. The first one is a smoothly varying macroscopic energy (the Coulomb and surface energies) calculated with the liquid drop model. The second one contains the shell  $E_{sh}$  and pairing corrections arising due to the shell structure of the nucleus.

The contribution of an odd nucleon, occupying a single-particle state  $|\mu\rangle$  with energy  $e_\mu$ , to the energy of a nucleus is described by the one-quasiparticle energy  $\sqrt{(e_\mu - e_F)^2 + \Delta^2}$ . Here the Fermi energy  $e_F$  and the pairing-energy gap parameter  $\Delta$  are calculated with in the BCS approximation. A pairing interaction of monopole type with the strength parameters  $G_p^n = (19.2 \mp 7.4 \frac{N-Z}{A})A^{-1}$  MeV [30] for neutrons and protons is used. For solving the pairing equations for  $e_F$  and  $\Delta$ , the same prescription as in Ref. [30] is used. In the calculations of  $e_F$  and  $\Delta$  the blocking effect [31] is not explicitly taken into consideration. To effectively take it into account in calculations of one-quasiparticle excitations

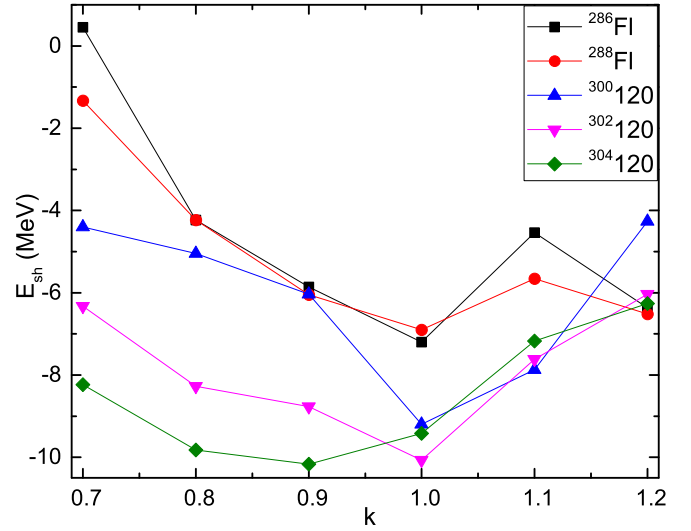


FIG. 1. The calculated shell-correction energies (symbols are connected by the lines) as functions of the coefficient  $k$  for  $^{286,288}\text{Fl}$  and  $^{300,302,304}\text{120}$  nuclei.

$E_\mu = \sqrt{(e_\mu - e_F)^2 + \Delta^2} - \sqrt{(e'_\mu - e_F)^2 + \Delta^2}$ , where  $e'_\mu$  is the single-particle energy of the occupied level just below the Fermi level, we use the results of Ref. [31], where the reduction of the calculated  $\Delta$  occurs by about a factor of 0.85. Calculating the potential energy surface as a function of collective coordinates with the TCSM, we find the ground-state potential minimum in which the energies of the low-lying one-quasiparticle states are obtained. The stability of SHN correlates with the shell correction energy  $E_{sh}$  in the ground state. The larger  $|E_{sh}|$  is, the greater the stability of SHN is with respect to spontaneous fission and  $\alpha$  decay.

### III. CALCULATED RESULTS

#### A. Position of shell closure

In this subsection, we try to understand the difference in predictions of proton shell closure in SHN. The fact that spin-orbit potential influences the positions of shells is known. The question is how. In order to study the influence of spin-orbit strength in the region of SHN with the modified TCSM, we take the spin-orbit term as  $kV_{ls}$  and study how the shell correction energies depend on the coefficient  $k$  varying from 0.8 to 1.2. The value  $k = 1$  corresponds to the parameters defined in Eqs. (4) and (5) [17,23,24].

The calculated shell corrections  $E_{sh}$  are presented in Fig. 1 as functions of  $k$  for the nuclei  $^{286,288}\text{Fl}$  and  $^{300,302,304}\text{120}$ . The smallest values of  $E_{sh}$  are achieved at  $k = 1.0$  for almost all nuclei. The only exception is  $^{304}\text{120}$ , which has a minimum value of  $E_{sh}$  at  $k = 0.9$ . So, the dependencies of  $E_{sh}$  on  $k$  show the minima at  $k \approx 1$  for both  $Z = 114$  and  $120$ . Note that the shell effects are stronger at  $Z = 120$  than at  $Z = 114$  in the case of  $0.7 \leq k \leq 1.1$ .

In Figs. 2–4, the values of shell correction energies are calculated using the spin-orbit strength of 0.8, 1, and 1.2 times previously fitted value [Eqs. (4) and (5)] [17,23,24] for

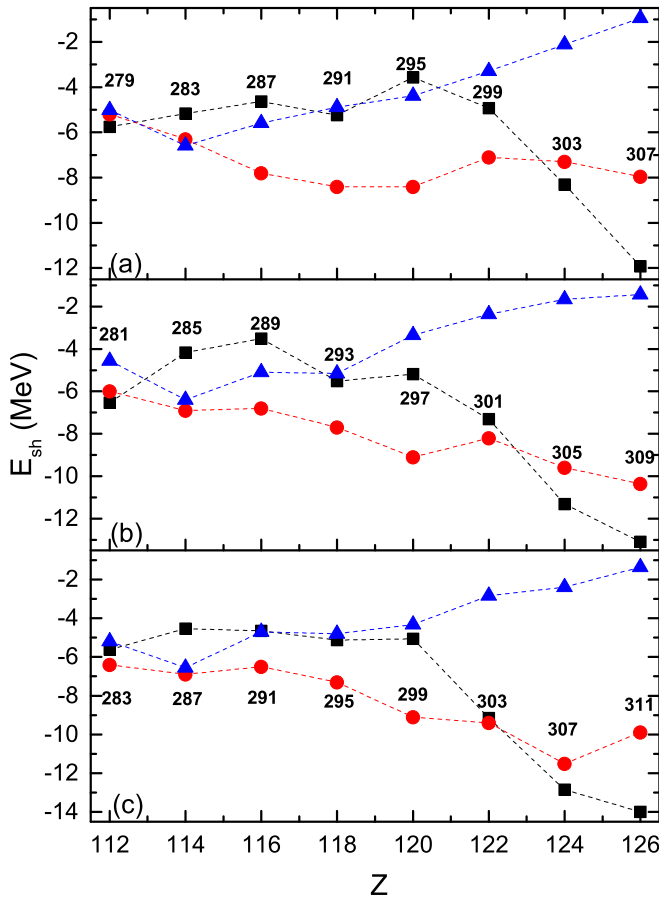


FIG. 2. The calculated values of shell corrections are presented for the nuclei of  $\alpha$ -decay chains containing  $^{295,297,299}120$ . The results are obtained at  $k = 0.8$  (squares),  $1.0$  (circles), and  $1.2$  (triangles). The mass numbers of nuclei are marked.

the SHN along the  $\alpha$ -decay chains containing  $^{295,297,299}120$ ,  $^{296,298,300}120$ , and  $^{302,304}120$ , respectively. At  $Z \leq 120$  and  $k = 1$ , we obtain the largest  $|E_{sh}|$  for most isotopes. The value of  $E_{sh}$  becomes more sensitive to  $k$  at  $Z > 120$ . While the value of  $E_{sh}$  goes up at  $k = 1.2$ , it goes down at  $k = 0.8$ . At  $k = 1.0$ , the isospin dependencies of  $E_{sh}$  is relatively weak for  $Z = 120$  and  $N \leq 180$  (Figs. 2 and 3). The stronger shell effects in  $^{302,304}120$  (Fig. 4) are related to the neutron shell at  $N = 184$ . In most cases the minimal value of  $E_{sh}$  corresponds to  $Z = 120$  at  $k = 1$ . If the neutron number approaches  $N = 184$ , the minimum is shifted to  $Z = 124$  or  $126$ . Thus, the shell effects are stronger at  $Z = 120$  than at  $Z = 114$  at  $k = 1$ .

Very pronounced minima of  $E_{sh}$  appear at  $Z = 126$  with decreasing  $k$  up to  $0.8$  (Figs. 2–4). Close values of  $E_{sh}$  for  $Z = 124$  and  $126$  in Figs. 2(c), 3(c), and 4 at  $k = 0.8$  reflect a strong role of the neutron shell at  $N = 184$ . The neutron shell at  $N = 174$  is pronounced only in  $^{291,292}\text{Og}$ . So, the weaker the spin-orbit strength is, the stronger the shell effects are at  $Z = 126$ .

For  $k = 1.2$ , there is a minimum of  $E_{sh}$  at  $Z = 114$  in all  $\alpha$ -decay chains considered (Figs. 2–4). Additional minima corresponding to the nuclei  $^{302,304}120$  appear due to the

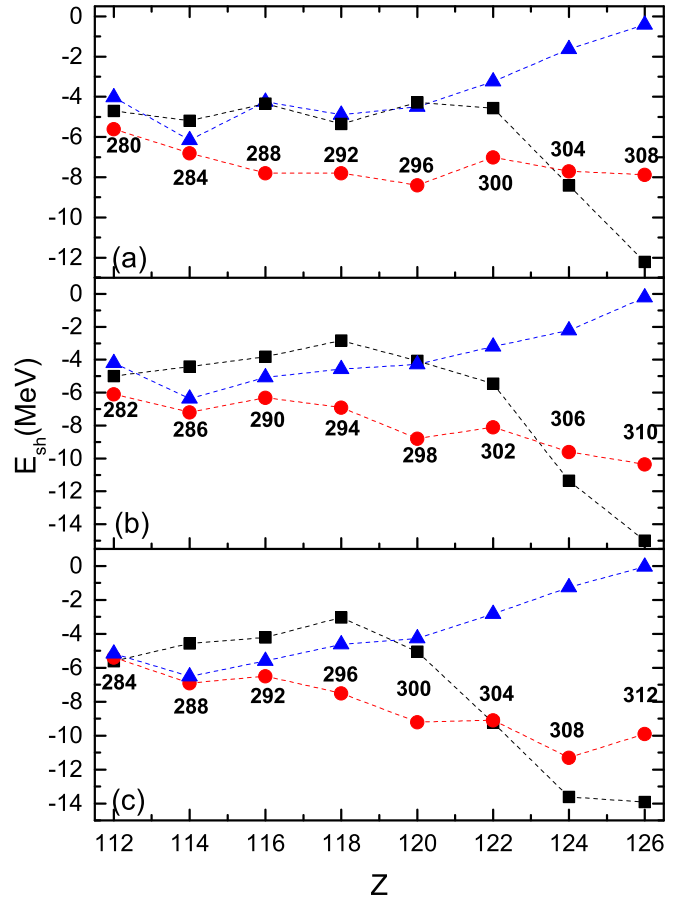


FIG. 3. The same as in Fig. 2, but for the nuclei of  $\alpha$ -decay chains containing  $^{296,298,300}120$ .

$N = 184$  shell. Note that the stability of the nuclei with  $Z > 120$  decreases with increasing  $k$ . The strength of spin-orbit interaction is crucial to define the position of the shell closures in nuclei beyond lead. The 20% variation of the spin-orbit strength can strongly shift the position of the minimum of  $E_{sh}$ .

The shape of the island of stability is mainly defined by the spin-orbit strength, a change of which by 20% leads to considerable changes. At  $k > 1$ , it is located between  $Z = 112$  and  $120$ , while at  $k \leq 1$  it is extended to  $Z = 126$ . The experiments on production of the  $Z = 120$  nucleus could help us to answer the question of where the center of island stability is located and whether there is a shelf of stability beyond  $Z = 120$ . Indeed, the properties of the  $Z = 120$  nucleus will reveal the stability/nonstability of nuclei with larger  $Z$ .

As mentioned in the Introduction, different models predict the proton shell either at  $Z = 114$  or at  $Z = 120$  and  $126$ . This difference in predictions seems to be related to the spin-orbit strengths used in the models. For example, a slight increase of the spin-orbit strength in Ref. [29] with respect to that in Ref. [27] results in the shift of the shell closure from  $Z = 120$  to  $Z = 114$ . In Refs. [29], it was proposed to extract the spin-orbital potential from the energy density functional used in the self-consistent calculations. The comparison of spin-orbit strengths in different models (MM, relativistic, and nonrelativistic mean-field models) can help us to understand

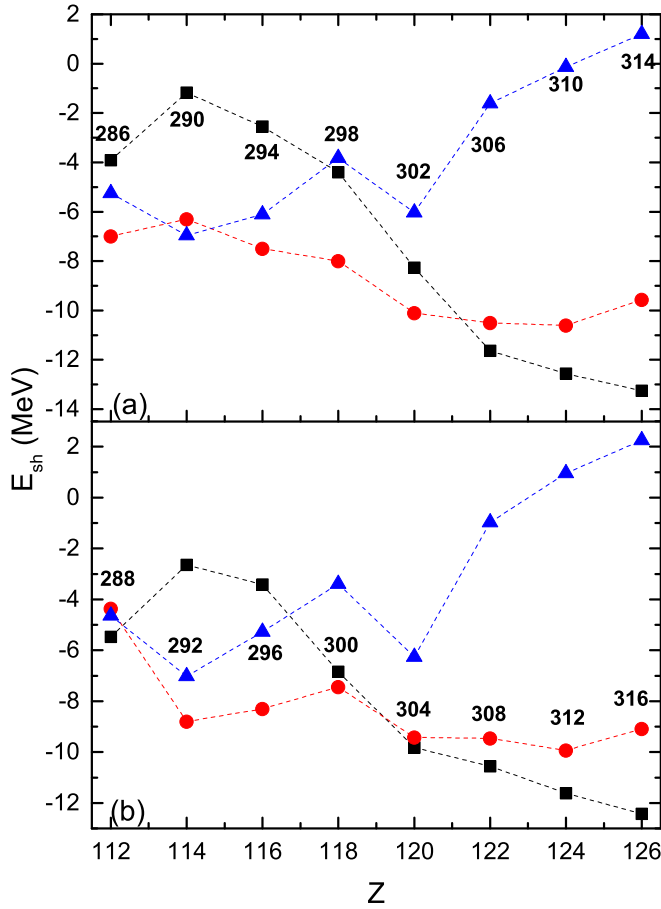


FIG. 4. The same as in Fig. 2, but for the nuclei of  $\alpha$ -decay chains containing  $^{302,304}120$ .

the variety of their predictions of proton shell closure in the region of SHN.

### B. Dependence of one-quasiparticle spectra on spin-orbit strength

To conclude on the reliability of the spin-orbit strength (the value of  $k$ ), we consider the spectra of low-lying one-quasiparticle states in heavy nuclei for which there are corresponding experimental data. As mentioned, the parameters of the TCSM were set at  $k = 1$  for the best description of the experimental one-quasiparticle spectra as well as the spins and parities of the ground states. In Figs. 5–8, the one-quasiparticle spectra calculated for  $^{251}\text{Cf}$ ,  $^{243}\text{Cm}$ ,  $^{243}\text{Bk}$ , and  $^{251}\text{Es}$  at  $k = 0.8, 1$ , and  $1.2$  are compared with the available experimental data [32]. The states are marked by the Nilsson asymptotic quantum numbers. Note that the experimental energies, spins, and parities are well described (within 250 keV) with  $k = 1.0$ . The calculated results obtained at  $k = 0.8$  and  $1.2$  are less consistent with the experimental data. In particular, the ground-state spins and parities cannot be reproduced. It should also be noted that the experimental isomeric state  $\frac{7}{2}^+$  in the  $^{251}\text{Cf}$  nucleus is reproduced in the calculation only at  $k = 1$ . An attempt to improve the description at  $k = 0.8$  and  $1.2$  by setting the parameter  $\mu$  in Eq. (3) failed. So a reason-

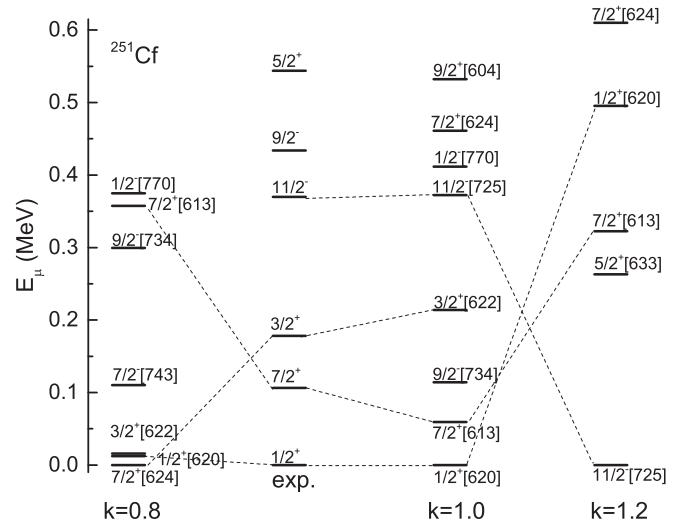


FIG. 5. The spectra of low-lying one-quasineutron states, calculated at indicated  $k$  for  $^{251}\text{Cf}$ , are compared with the available experimental data [32]. The states are marked by the Nilsson asymptotic quantum numbers.

able change in the value of  $V_{l2}$  does not improve the low-lying spectrum at  $k \neq 1$ . The best description of the structure of actinides and transactinides at  $k = 1$  corresponds to stronger shell effects at  $Z = 120$  although shell effects at  $Z = 114$  are also pronounced.

In most cases, the one-quasiparticle spectra become denser if the value of  $k$  deviates from 1. We found that at  $k = 0.9$  the calculated ground-state spins are still in good agreement with the experimental assignments, but the higher energy levels do not fit the data. At  $k = 1.1$ , there are shifts of the levels with low spin upward and the states with large spin downward. Thus, at  $k = 1$  we have the best description of low-lying one-quasiparticle states of actinides and the strongest shell effects for nuclei with  $Z \leq 120$ . It seems that the quasiparticle structure of actinides contains some information about the next double magic nucleus beyond  $^{208}\text{Pb}$ . So, the nuclear

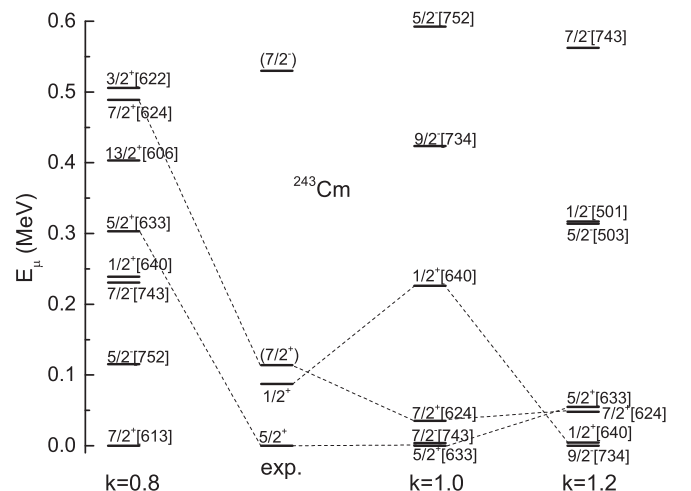


FIG. 6. The same as in Fig. 5, but for  $^{243}\text{Cm}$ .

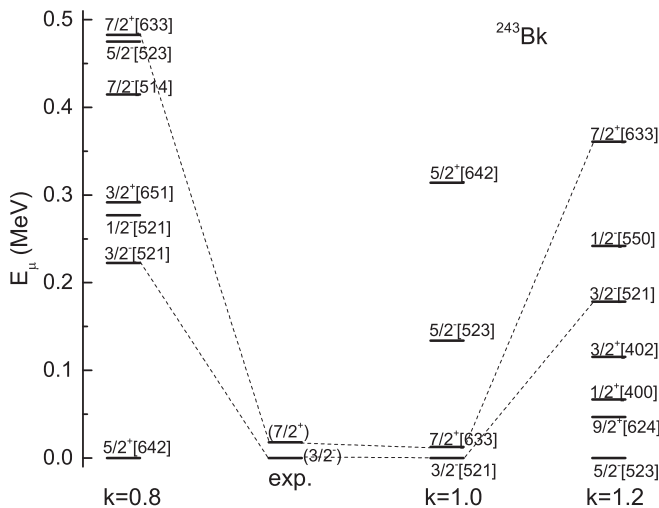


FIG. 7. The spectra of low-lying one-quasiproton states, calculated at indicated  $k$  for  $^{243}\text{Bk}$ , are compared with the available experimental data [32]. The states are marked by the Nilsson asymptotic quantum numbers.

spectroscopic investigations are important in the region of actinides and transactinides for reliable prediction of the proton shell in SHN. The intensive study of structure of heavy nuclei allows us to define the parameters of microscopic approaches and reliably predict the shell effects in SHN.

#### IV. SUMMARY

At the spin-orbit strength ( $k = 1$ ) taken in the modified TCSM the strongest shell effects are found for the nuclei with  $Z = 120$ , or with 124 and 126 at  $N$  approaching 184. However, the variation of the value of  $E_{sh}$  in the isospin chains is relatively small, which confirms the results of self-consistent calculations [27,28]. With decreasing spin-orbit strength ( $k = 0.8$ ) the proton shell closure is shifted to  $Z = 126$ . For larger spin-orbit interaction ( $k = 1.2$ ), the nuclei with  $Z = 114$  are calculated to have the largest values of shell-correction energy. The shell effect at  $N = 184$  is quite strong and interplays with proton shell effects while the shell effect at  $N = 174$  is less pronounced. So, the 20% variation of the spin-orbit

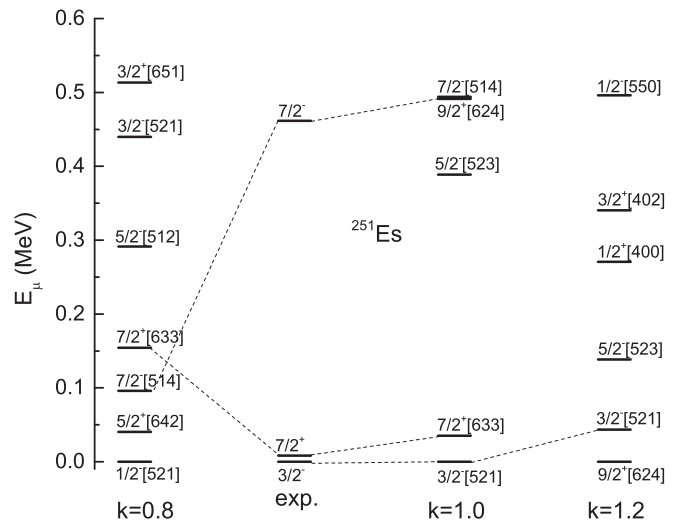


FIG. 8. The same as in Fig. 7, but for  $^{251}\text{Es}$ .

strength can strongly shift the center of island stability. By extracting the mean-field potentials from the energy density functionals used in the self-consistent approaches and comparing them with those in the MM models, one can understand the difference in predictions of proton shell closure in SHN.

As shown, the quality of the description of low-lying one-quasiparticle states of actinides crucially depends on the spin-orbit strength. The spin-orbit strength at  $k = 1$  allows us to describe well the low-lying one-quasiparticle spectra in heavy nuclei [17,23,24]. At  $k = 0.8$  and 1.2 the calculated spectra are less consistent with the experimental data. Note that at  $k = 1$  we have also the strongest shell effects for nuclei with  $Z \leq 120$ . So, the nuclear structure of actinides contains some information about the next double magic nucleus beyond  $^{208}\text{Pb}$ , and studies of the structure of the heaviest nuclei allow us to define the parameters of the nuclear mean field and reliably predict the shell effects in still unknown SHN.

#### ACKNOWLEDGMENTS

G.G.A. and N.V.A. were supported by the Ministry of Science and Higher Education of the Russian Federation (Contract No. 075-10-2020-117).

[1] Yu. Ts. Oganessian, *J. Phys. G* **34**, R165 (2007).

[2] Yu. Ts. Oganessian, F. S. Abdullin, P. D. Bailey, D. E. Benker, M. E. Bennett, S. N. Dmitriev, J. G. Ezold, J. H. Hamilton, R. A. Henderson, M. G. Itkis, Y. V. Lobanov, A. N. Mezentsev, K. J. Moody, S. L. Nelson, A. N. Polyakov, C. E. Porter, A. V. Ramayya, F. D. Riley, J. B. Roberto, M. A. Ryabinin *et al.*, *Phys. Rev. Lett.* **104**, 142502 (2010); *Phys. Rev. C* **87**, 014302 (2013); **87**, 034605 (2013); **87**, 054621 (2013); V. K. Utyonkov, N. T. Brewer, Yu. Ts. Oganessian, K. P. Rykaczewski, F. S. Abdullin, S. N. Dmitriev, R. K. Grzywacz, M. G. Itkis, K. Miernik, A. N. Polyakov, J. B. Roberto, R. N. Sagaidak, I. V. Shirokovsky, M. V. Shumeiko, Y. S. Tsyganov,

A. A. Voinov, V. G. Subbotin, A. M. Sukhov, A. V. Sabelnikov, G. K. Vostokin, J. H. Hamilton, M. A. Stoyer, and S. Y. Strauss, *Phys. Rev. C* **92**, 034609 (2015); **97**, 014320 (2018).

[3] Yu. Ts. Oganessian and V. K. Utyonkov, *Nucl. Phys. A* **944**, 62 (2015); *Rep. Prog. Phys.* **78**, 036301 (2015).

[4] S. Hofmann *et al.*, *Eur. Phys. J. A* **32**, 251 (2007); **48**, 62 (2012); **52**, 180 (2016).

[5] S. Hofmann, in *The Euroschool Lectures on Physics with Exotic Beams, Vol. III*, Lecture Notes in Physics Vol. 764 (Springer, Berlin, 2009), p. 203.

[6] S. Heinz *et al.*, *J. Phys.: Conf. Ser.* **282**, 012007 (2011).

[7] R. Eichler *et al.*, *Nature (London)* **447**, 72 (2007).

- [8] L. Stavsetra, K. E. Gregorich, J. Dvorak, P. A. Ellison, I. Dragojević, M. A. Garcia, and H. Nitsche, *Phys. Rev. Lett.* **103**, 132502 (2009).
- [9] C. E. Düllmann, M. Schädel, A. Yakushev, A. Türler, K. Eberhardt, J. V. Kratz, D. Ackermann, L. L. Andersson, M. Block, W. Brüche, J. Dvorak, H. G. Essel, P. A. Ellison, J. Even, J. M. Gates, A. Gorshkov, R. Graeger, K. E. Gregorich, W. Hartmann, R.-D. Herzberg *et al.*, *Phys. Rev. Lett.* **104**, 252701 (2010); J. M. Khuyagbaatar *et al.*, *ibid.* **112**, 172501 (2014).
- [10] J. M. Gates, C. E. Düllmann, M. Schädel, A. Yakushev, A. Türler, K. Eberhardt, J. V. Kratz, D. Ackermann, L. L. Andersson, M. Block, W. Brüche, J. Dvorak, H. G. Essel, P. A. Ellison, J. Even, U. Forsberg, J. Gellanki, A. Gorshkov, R. Graeger, K. E. Gregorich *et al.*, *Phys. Rev. C* **83**, 054618 (2011).
- [11] S. Hofmann and G. Münzenberg, *Rev. Mod. Phys.* **72**, 733 (2000).
- [12] K. Morita *et al.*, *J. Phys. Soc. Jpn.* **73**, 2593 (2004); **76**, 043201 (2007); *Eur. Phys. J. A* **21**, 257 (2004).
- [13] G. G. Gulbekian *et al.*, *Phys. Part. Nucl. Lett.* **16**, 866 (2019).
- [14] P. Möller, J. R. Nix, W. D. Myers, and W. J. Swiatecki, *At. Data Nucl. Data Tables* **59**, 185 (1995).
- [15] I. Muntian, Z. Patyk, and A. Sobiczewski, *Acta. Phys. Pol. B* **32**, 691 (2001); **34**, 2141 (2003); **34**, 2073 (2003); I. Muntian, S. Hofmann, Z. Patyk, and A. Sobiczewski, *Phys. At. Nucl.* **66**, 1015 (2003); A. Parkhomenko, I. Muntian, Z. Patyk, and A. Sobiczewski, *Acta. Phys. Pol. B* **34**, 2153 (2003); A. Parkhomenko and A. Sobiczewski, *ibid.* **36**, 3115 (2005).
- [16] M. Kowal and J. Skalski, *Phys. Rev. C* **82**, 054303 (2010); **85**, 061302(R) (2012); P. Jachimowicz, M. Kowal, and J. Skalski, *ibid.* **85**, 034305 (2012); **89**, 024304 (2014); **95**, 014303 (2017); **101**, 014311 (2020); *At. Data Nucl. Data Tables* **138**, 101393 (2021).
- [17] G. G. Adamian, N. V. Antonenko, and W. Scheid, *Phys. Rev. C* **81**, 024320 (2010); **82**, 054304 (2010).
- [18] P. G. Reinhard, *Rep. Prog. Phys.* **52**, 439 (1989).
- [19] P. Ring, *Prog. Part. Nucl. Phys.* **37**, 193 (1996).
- [20] M. Bender, P. H. Heenen, and P. G. Reinhard, *Rev. Mod. Phys.* **75**, 121 (2003).
- [21] J. Meng, H. Toki, S. G. Zhou, S. Q. Zhang, W. H. Long, and L. S. Geng, *Prog. Part. Nucl. Phys.* **57**, 470 (2006).
- [22] G. G. Adamian, N. V. Antonenko, S. N. Kuklin, B. N. Lu, L. A. Malov, and S. G. Zhou, *Phys. Rev. C* **84**, 024324 (2011); A. Taninah, S. E. Agbemava, and A. V. Afanasjev, *ibid.* **102**, 054330 (2020); Z. Shi, A. V. Afanasjev, Z. P. Li, and J. Meng, *ibid.* **99**, 064316 (2019).
- [23] A. N. Kuzmina, G. G. Adamian, and N. V. Antonenko, *Eur. Phys. J. A* **47**, 145 (2011).
- [24] A. N. Kuzmina, G. G. Adamian, N. V. Antonenko, and W. Scheid, *Phys. Rev. C* **85**, 014319 (2012).
- [25] J. Maruhn and W. Greiner, *Z. Phys. A* **251**, 431 (1972).
- [26] S. Liran, A. Marinov, and N. Zeldes, *Phys. Rev. C* **62**, 047301 (2000).
- [27] G. G. Adamian, N. V. Antonenko, H. Lenske, L. A. Malov, and S.-G. Zhou, *Eur. Phys. J. A* **57**, 89 (2021).
- [28] G. G. Adamian, L. A. Malov, N. V. Antonenko, H. Lenske, K. Wang, and S.-G. Zhou, *Eur. Phys. J. A* **54**, 170 (2018).
- [29] L. A. Malov, G. G. Adamian, N. V. Antonenko, and H. Lenske, *Phys. Rev. C* **104**, L011304 (2021); **104**, 064303 (2021).
- [30] S. G. Nilsson, C. F. Tsang, A. Sobiczewski, Z. Szymanski, S. Wycech, Ch. Gustafson, I.-L. Lamm, P. Möller, and B. Nilsson, *Nucl. Phys. A* **131**, 1 (1969).
- [31] V. G. Soloviev, *Theory of Complex Nuclei* (Pergamon Press, Oxford, 1976).
- [32] <https://www.nndc.bnl.gov>.